

UDC 624.012
DOI: 10.15587/1729-4061.2020.194145

Для суттєвого зменшення ваги плоских монолітних залізобетонних перекриттів, фундаментів та інших плитних конструкцій все ширше застосовують в практиці будівництва ефективні вставки як окремі вироби з відносно легких і дешевих матеріалів, які розташовують в середній частині перерізу і залишають у плитах після їх бетонування.

Вставки з відносно легких і дешевих матеріалів по відношенню до бетону мають на порядки меншу міцність та жорсткість, і є по суті порожниноутворюючими. Розглянуті вставки є призматичними. За розташування вставок у двох напрямках, що є характерним для більшості плитних конструкцій, отримуємо двотаврові перерізи, при розрахунку яких проаналізовано вплив загальних і місцевих силових факторів. За таких умов плити необхідно розраховувати з врахуванням двовісної роботи бетону. В статті розглянуто напружено-деформований стан плитних залізобетонних конструкцій з двонаправленим розташуванням вставок, а також подано обґрунтування розрахункових схем та розрахункові залежності, що стосуються методики розрахунку перекриттів та інших плитних залізобетонних конструкцій з двонаправленим розташуванням вставок. Наведено приклад розрахунку монолітного перекриття за запропонованою методикою, який показав, що врахування двовісного напружено-деформованого стану бетону суттєво збільшує міцність бетону і жорсткість перекриття – на 19,3 %.

Отже, врахування двовісного стиску бетону є важливим чинником при проектуванні плитних конструкцій з двонаправленим розташуванням вставок

Ключові слова: залізобетонні порожнисті плитні конструкції, напружено-деформований стан, двовісний стиск бетону, розрахункові схеми, міцність, жорсткість, приклад розрахунку

THE STRESSED-DEFORMED STATE OF SLAB REINFORCED-CONCRETE HOLLOW STRUCTURES CONSIDERING THE BIAXIAL COMPRESSION OF CONCRETE

A. Bambura

Doctor of Technical Sciences, Professor
Department of Reliability of Building Structures
State Enterprise «State Research Institute of Building Constructions»
Preobrazhenska str., 5/2, Kyiv, Ukraine, 03037
E-mail: abambura@gmail.com

I. Mel'nyk

PhD, Associate Professor*
E-mail: GNDL112@ukr.net

V. Bilozir

PhD, Associate Professor
Department of Building Structures
Lviv National Agrarian University
V. Velykoho str., 1, Dubliany, Zhovkva district,
Lviv reg., Ukraine, 80381
E-mail: bilozir.vitaly@ukr.net

V. Sorokhtey

Senior Researcher
Branch Research Laboratory No. 112**
E-mail: monza@ukr.net

T. Prystavskiy

Senior Researcher
Branch Research Laboratory No. 112**
E-mail: taras.vol@ukr.net

V. Partuta*

E-mail: vova.partuta@gmail.com
*Department of Building Constructions and Bridges**
**Lviv Polytechnic National University
S. Bandery str., 12, Lviv, Ukraine, 79013

Received date 21.10.2019

Accepted date 27.01.2020

Published date 24.02.2020

Copyright © 2020, A. Bambura, I. Mel'nyk, V. Bilozir, V. Sorokhtey, T. Prystavskiy, V. Partuta

This is an open access article under the CC BY license

(<http://creativecommons.org/licenses/by/4.0>)

1. Introduction

Construction operations have increasingly exploited monolithic reinforced concrete floors and other slab structures with effective inserts whose application yields a significant reduction in the natural weight of slabs, thereby saving concrete and reinforcement fittings [1].

While the plastic inserts of various shapes are mainly used abroad, operations in Ukraine involve prismatic polystyrene inserts that have the one-way (one direction) or two-way arrangement of inserts.

Under conditions of arranging the inserts in both directions, which is characteristic of most slab structures, it is necessary to take into consideration the biaxial stressed-

strained state of concrete; however, the current calculation procedures do not account for it.

2. Literature review and problem statement

Paper [2] considers the impact of a dynamic load on the strength, deformability, and micro-crack-formation of concrete at its uni- and biaxial compression. Study [3] reports the orthotropic model of concrete under the biaxial and triaxial dynamic load. Articles [4, 5] describe the results of studying a high-speed dynamic load. However, similarly to work [2], the established dynamic influences are not characteristic of the slab reinforced concrete structures considered.

Based on the results from [6], a model was proposed describing the stress and deformation ratio at biaxial compression. However, it relates to recycled concrete and cannot be used for standard concrete. A study into the biaxial compression [7] was carried out using a special device that allowed control over the deformation mode by changing the characteristics of rigidity. However, the results obtained can be used only to analyze methods for calculating statically undefined systems.

A twelve-year investigation into concrete exposed to a biaxial load demonstrated that the Poisson's coefficient of creep is approximately constant over time while the Young's module increases considerably [8]. However, the analytical description of these changes, given in the paper, is difficult to use.

Study [9] tested the biaxially stressed concrete of significant strength – from 58 to 94 MPa. However, the resulting values of stress coefficients cannot be used for slab reinforced concrete structures, the concrete strength of which is 2...3 times less than the experimental concrete. Based on the results of testing cubic samples (10×10×10 cm), study [10] substantiated the criteria for concrete failure at biaxial and triaxial compression. However, the proposed five- and six-parametric models of concrete strength are difficult to use in engineering calculations. The experimental-theoretical study of concrete deformation exposed to the biaxially-stressed state [11] considered only concrete and was used for the calculation of beams lying on a pliable base.

Proposals for calculating the monolithic flat reinforced concrete floors and other slab structures with a unidirectional arrangement of inserts, given in paper [12], relate to determining the rigidity characteristics of slabs in both directions during their general static calculation, but excluding the modified characteristics of concrete.

Our analysis of the literary sources allows one to conclude that there are neither justified estimation schemes nor analysis of the stressed-strained state, which could be used to calculate slab structures with a bidirectional arrangement of inserts considering the biaxial work of concrete.

3. The aim and objectives of the study

The aim of this study is to substantiate the estimation schemes of flat slab hollow structures with a bidirectional arrangement of inserts taking into consideration the stressed-strained state of concrete exposed to biaxial compression in order to devise a procedure for their calculation.

To accomplish the aim, the following tasks have been set:

- to justify estimation schemes reflecting the stressed-strained state of structures with a bidirectional arrangement of inserts;

- to review and analyze estimation dependences that describing the biaxial state of concrete;
- to demonstrate the application of the devised procedure in practice using an example.

4. Substantiation of estimation schemes

Most structural solutions for reinforced concrete slabs with inserts employ the square or rectangular outlines with the appropriate interperpendicular internal arrangement of intermediate beams-edges, that is the orthotropic slab structures. Their estimation scheme must consider and analyze the presence of general and local strength factors.

Consider this using an example of the flooring slab with rectangular inserts, part of which is shown in Fig. 1.

In the general design of the slab, we have, in the vicinity of the cross-section of beams, the I-sections in each direction (directions *X* and *Y* – Fig. 2), hereafter, the I-sections. When calculating the crack formation, we use an I-section (Fig. 2, *a*); when calculating for the bearing capacity – a conditional T-section (Fig. 2, *b*).

In the upper shelf of the flooring slab, this being an uncut structure, the middle (interbeam) part is exposed to the momenta that stretch the lower fibers of the shelf, thereby squeezing the upper zone.

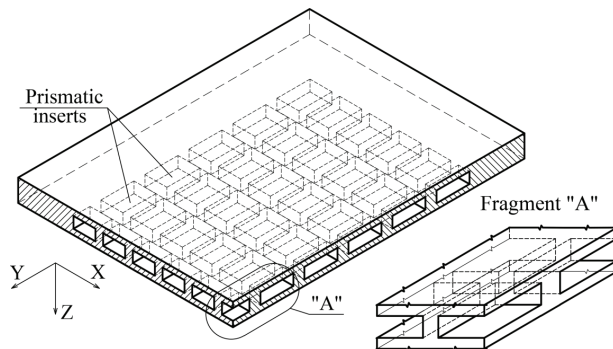


Fig. 1. Part of the monolithic flat reinforced concrete slab with prismatic inserts

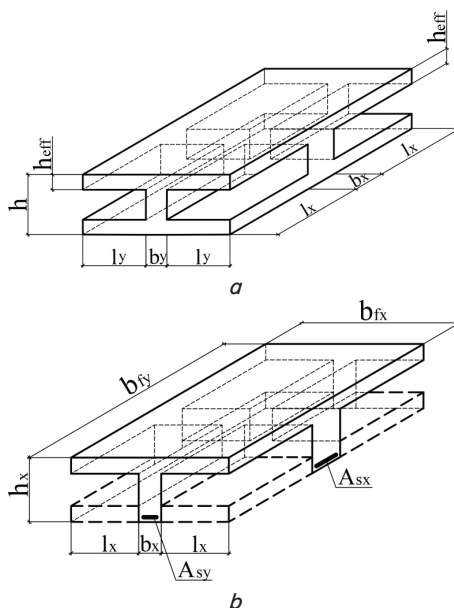


Fig. 2. I-section: *a* – actual; *b* – estimated

Near and above the beams, the shelf experiences the momenta of the opposite direction (sign), which induce the forces that stretch the upper fibers of the shelf and, consequently, compress its lower zone (Fig. 3, a, b).

However, the stretching effort per unit length N_{s1}^x of the shelves, following the equilibrium conditions, is equal to a similar compressing effort N_{b1}^x (Fig. 3, c). Similarly, $N_{s1}^y = N_{b1}^y$, which is why these pairs of efforts are mutually balanced and in the projection onto the horizontal axis are equal to zero.

Thus, the estimation scheme of the upper shelves retains the compressing stresses σ_y and σ_x due to the action of general momenta M_x, M_y (Fig. 3, d).

Possible cases of the estimation diagrams for an I-section are shown in Fig. 4:

- the neutral axis of the I-section in the X and Y directions is in the edge (Fig. 4, a);
- the neutral axis in the Y direction is in the edge, and in the X direction – in the shelf (Fig. 4, b);
- the neutral axis in the Y direction is in the shelf, in the X direction – in the edge (Fig. 4, c);
- the neutral axis in the X and Y directions passes the shelves (Fig. 4, d).

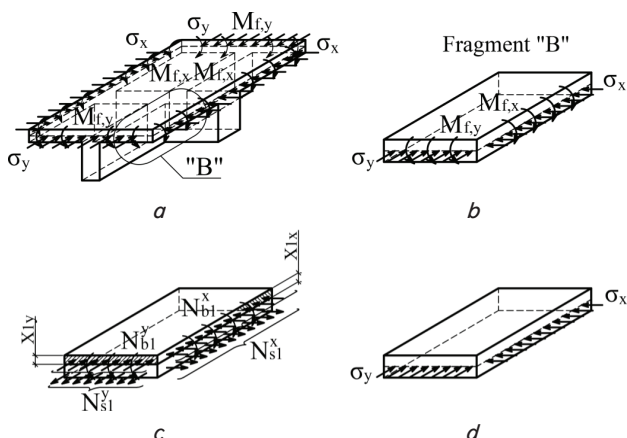


Fig. 3. The stressed state of the shelves of an I-section (in Fig. 3, b–d, the efforts and stresses on the opposite sides are not shown): a – general stressed state of the cross-section; b – fragment «B»; c – efforts in the shelf due to momenta; d – stresses in the shelf

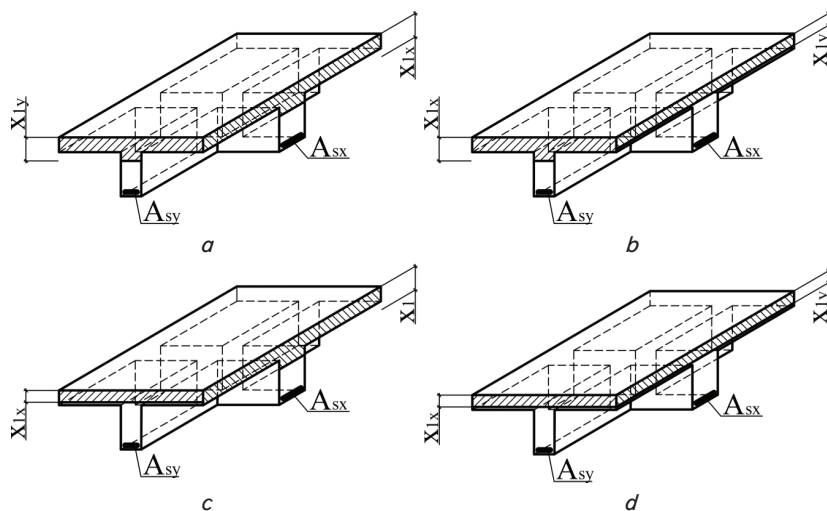


Fig. 4. Estimation schemes of the I-section: a – neutral axis is in the edges; b, c – neutral axis is in the edge and the shelf; d – neutral axis is in the shelf

The estimation scheme is chosen in the calculation process for each case.

5. Estimation dependences of the biaxial compression of concrete

A comprehensive study of the concrete compressed in both directions that was conducted at the DP State Scientific and Research Institute of Building Structures (Kyiv, Ukraine) [11] has shown that under conditions of a biaxial state a positive effect is observed on the boundary strength and deformation properties of concrete. Thus, the strength of concrete increases by 16...30 % (Fig. 5), the deformations – by 23...56 % (Fig. 6), depending on the level of the second component of stresses in concrete σ_{b2} .

Based on the results from our experimental study, and with a reference to the studies by other authors [13], the following dependences were derived [11]:

$$\frac{\hat{\sigma}_{b1}}{f_{cd}} = 1 + 1.38 \frac{\sigma_{b2}}{f_{cd}} - 1.15 \left(\frac{\sigma_{b2}}{f_{cd}} \right)^2, \tag{1}$$

$$\frac{\hat{\epsilon}_{b1}}{\epsilon_{bR}} = 1 + 2.15 \frac{\sigma_{b2}}{f_{cd}} - 1.95 \left(\frac{\sigma_{b2}}{f_{cd}} \right)^2, \tag{2}$$

in which:

- $\hat{\sigma}_{b1} = f_{cd}$ and $\hat{\epsilon}_{b1} = \epsilon_{bR}$ at $\sigma_{b2} / f_{cd} = 0$;
- $\hat{\sigma}_{b1} = 1.3 f_{cd}$ and $\hat{\epsilon}_{b1} = 1.56 \epsilon_{bR}$ at $\sigma_{b2} / f_{cd} = 0.4$;
- $\hat{\sigma}_{b1} = 1.15 f_{cd}$ and $\hat{\epsilon}_{b1} = 1.23 \epsilon_{bR}$ at $\sigma_{b2} / f_{cd} = 1.0$.

In these dependences:

- $\hat{\sigma}_{b1}$ – boundary values of the principal (greater) compressive stress σ_{b1} ;
- f_{cd} – estimation value of concrete strength for compression;
- $\hat{\epsilon}_{b1}$ – deformations of concrete, corresponding to its maximum strains along the direction of a greater compressive effort (boundary values of relative deformations of concrete for stress $\hat{\sigma}_{b1}$);
- ϵ_{bR} – boundary deformations of concrete under a uniaxial compression;
- σ_{b2} – transverse (perpendicular) compressive stress to σ_{b1} (the second component of stresses).

When this approach is used, one applies the experimental, normative, or estimation values for the coefficient of the polynomial in the axial compression diagram.

Acting construction standards (DBN V.2.6-98:2009) also take into consideration that under a biaxial compression one achieves the higher strength of concrete and the greater critical deformations. However, in contrast to proposals [11], the dependence of concrete deformation and strain was adopted in a simpler form – two-linear with rectilinear plots (Fig. 7).

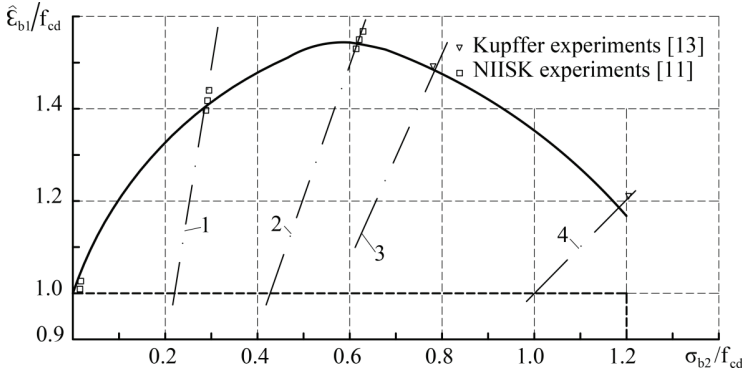


Fig. 5. Boundary curve of concrete deformation under biaxial state: 1 – $\sigma_2=0.2\sigma_1$; 2 – $\sigma_2=0.4\sigma_1$; 3 – $0.52\sigma_2$; 4 – $\sigma_2=\sigma_1$

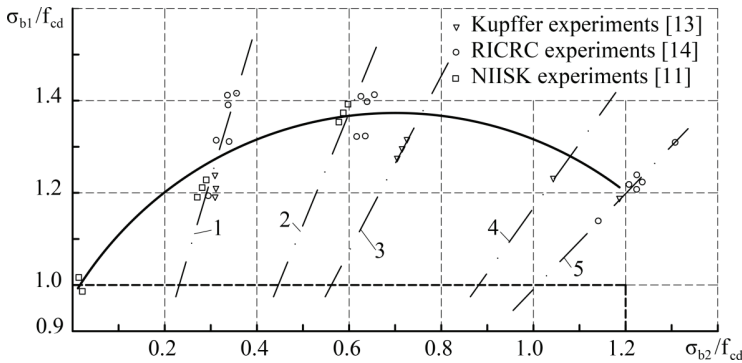


Fig. 6. Boundary curve of concrete strength under biaxial state: 1 – $\sigma_2=0.2\sigma_1$; 2 – $\sigma_2=0.4\sigma_1$; 3 – $\sigma_2=0.52\sigma_1$; 4 – $\sigma_2=0.83\sigma_1$; 5 – $\sigma_1=\sigma_2$

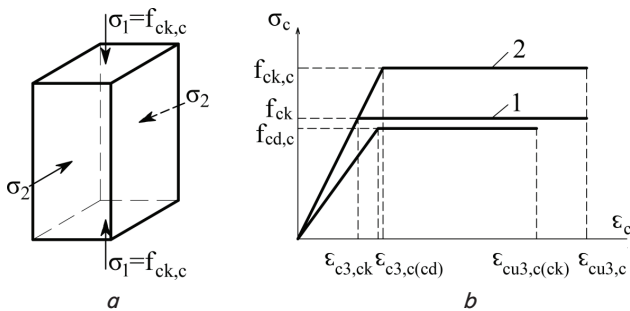


Fig. 7. Dependence of the stresses and deformation of concrete under the two-dimensional compression of the non-compressed (1) concrete and compressed (2) concrete: a – general scheme of biaxial stress; b – dependence $\sigma_c - \epsilon_c$

According to DBN V.2.6-98:2009, the dependences between the stresses and deformation of concrete under its biaxial compression are as follows:

$$f_{ck,c} = f_{ck} \left[1.0 + 1.38 \frac{\sigma_2}{f_{ck}} - 1.15 \left(\frac{\sigma_2}{f_{ck}} \right)^2 \right] \quad (3)$$

for $0 < \sigma_2 / f_{ck} \leq 1.0 f_{ck}$,

$$\epsilon_{cu3,c} = f_{ck,c} / E_{ck}, \quad (4)$$

$$\epsilon_{cu3,c} = \epsilon_{cu3}, \quad (5)$$

where σ_2 are the actual transverse stresses of compression in the general coordinates, due to compression; ϵ_{c3} , ϵ_{cu3} and

E_{ck} are the values of relative deformations and the module of concrete elasticity, selected according to Table 3.1 from DBN V.2.6-98:2009.

As one can see, underlying formula (3) are the dependences recommended in work [11]; however, in this case, it is not the characteristic (normative) strength of concrete for compression used, but the estimated strength of concrete for compression.

6. Example of the calculation of prisms taking into consideration the biaxial compression of concrete

6.1. Source data

The chosen example is a flooring slab with polystyrene inserts, whose fragment is shown in Fig. 8. General dimensions of the slab fragment (the distances between the axes of columns in the x and y directions) are 6.86×6.06 m.

The inserts have plan dimensions of 0.5×1 m, forming the edges in both directions with a thickness of 10 cm. Given the thickness of the inserts of 10 cm and the total height of the flooring slab of 20 cm, the thickness of the upper and lower shelves was adopted the same, 5 cm each (Fig. 8).

According to the requirements by DBN V.2.6-98:2009, the working width of the shelves for all boundary states is determined from formula:

$$b_{eff} = 2b_{eff,1} + b_w, \quad (6)$$

where $b_{eff,1}$ is the estimation width of the shelf, determined from condition:

$$b_{eff,1} = 0.2b_1 + 0.1l_0 \leq 0.2l_0 \leq b_1,$$

$$b_{eff,1} < b_1. \quad (7)$$

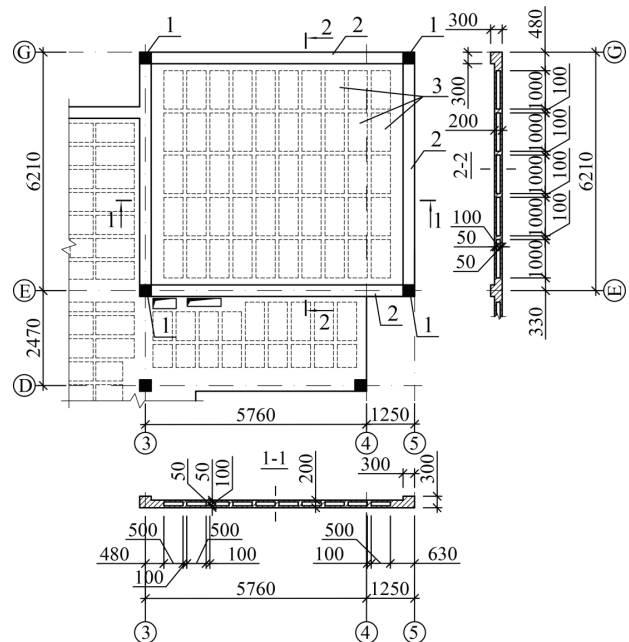


Fig. 8. Fragment of a monolithic reinforced concrete flooring slab with prismatic inserts: 1 – columns; 2 – contour beams; 3 – inserts

In dependences (6) and (7): b_w – the width of the edge; b_1 – the estimation width of an overhang (console), l_0 – the estimation length. Under conditions of pinching in the contour beams $l_0 = 0.7l$.

Taking into consideration these recommendations, we calculate the working width of the shelves of an I-section in the X and Y directions.

6. 2. Determining the working width of the shelf in the X direction

The estimated distance (Fig. 9):

$$l_0^x = 0.7l^x = 0.7 \cdot 6.86 = 4.8 \text{ m.}$$

$$b_1^x = \frac{0.5}{2} = 0.25 \text{ m;}$$

$$b_{eff,1}^x = 0.2b_1^x + 0.1l_0^x = 0.2 \cdot 0.25 + 0.1 \cdot 4.8 = 0.53 \text{ m} > b_1^x = 0.25 \text{ m;}$$

$$b_{eff,1}^x = 0.53 \text{ m} < 0.2l_0^x = 0.2 \cdot 4.8 = 0.96 \text{ m;}$$

Accept $b_{eff,1}^x = 0.25 \text{ m.}$

Accordingly, $b_{eff}^x = 2b_{eff,1}^x + b_w^x = 2 \cdot 0.25 + 0.1 = 0.6 \text{ m.}$

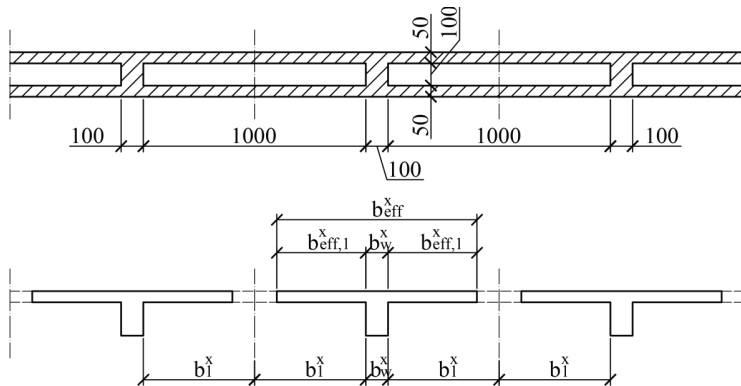


Fig. 9. Determining the working width of the shelf in the X direction

6. 3. Determining the working width of the shelf in the Y direction

The estimated distance (Fig. 10):

$$l_0^y = 0.7 \cdot 6.06 = 4.24 \text{ m;}$$

$$b_1^y = \frac{1}{2} = 0.5 \text{ m;}$$

$$b_{eff,1}^y = 0.2b_1^y + 0.1l_0^y = 0.2 \cdot 0.5 + 0.1 \cdot 4.24 = 0.524 \text{ m} > b_1^y = 0.5 \text{ m;}$$

$$b_{eff,1}^y = 0.524 \text{ m} < 0.2l_0^y = 0.2 \cdot 4.24 = 0.85 \text{ m.}$$

Accept $b_{eff,1}^y = 0.5 \text{ m.}$

Accordingly, $b_{eff}^y = 2b_{eff,1}^y + b_w^y = 2 \cdot 0.5 + 0.1 = 1.1 \text{ m.}$

In addition to the geometric parameters, the source data for calculating the standard I-sections are the values of bending momenta in both directions (M_x, M_y).

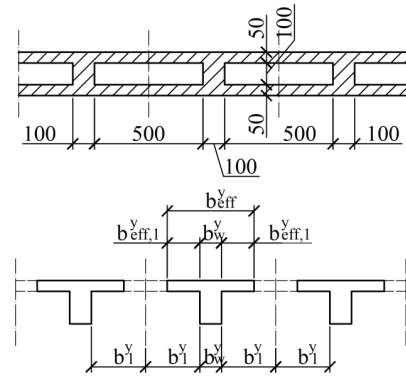


Fig. 10. Determining the working width of the shelf in the Y direction

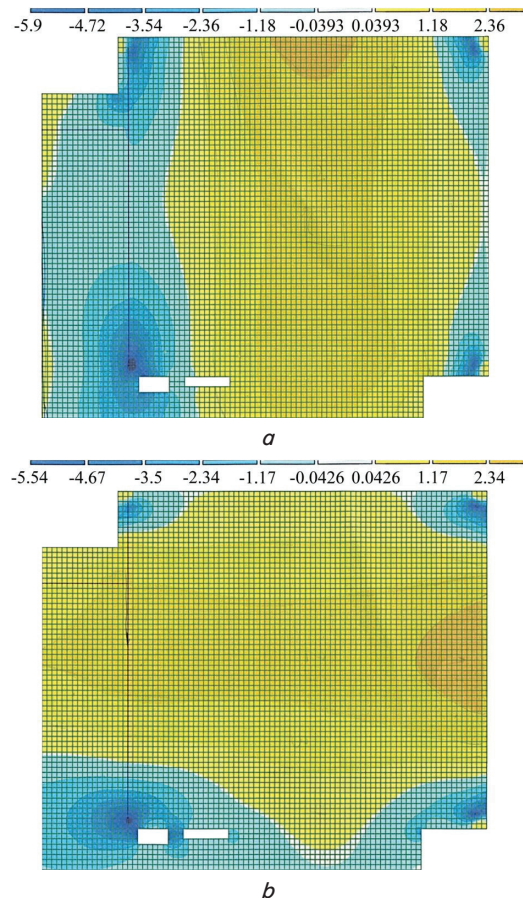


Fig. 11. Contour plots of change in momenta: a – in the X direction; b – in the Y direction

In this case, the values of M_x, M_y were chosen according to the results from the general statistical calculation of a flooring slab as part of the frame of a building in the software package LIRA Sapr13 with the use of shell elements and linear elements (Fig. 11).

6. 4. Determining the required amount of longitudinal working reinforcement fittings

To determine the required amount of longitudinal working reinforcement fittings, we use recommendations from [15] provided the neutral axis does not go beyond the compressed shelf of an I-section. Under other circumstances, we apply the recommendations from [16].

The required amount of reinforcement fittings, in accordance with the guidelines from [15], can be calculated from equation (8), pre-defining the magnitude of discriminant D in square equation (9), to solve it, and the height of the compressed zone considering the coefficient $\lambda = 0.8$:

$$b\lambda f_{cd}x_1 - A_s f_{yd} = 0, \tag{8}$$

$$-\lambda x_1^2 + 2Ad_0x_1 - 2\frac{M_{Ed}}{b\lambda f_{cd}} = 0; \tag{9}$$

$$D = 4d_0^2 - \frac{8M_{Ed}}{b\lambda f_{cd}}; \tag{10}$$

$$x_1 = \frac{-2d_0 \pm \sqrt{D}}{-2\lambda}. \tag{11}$$

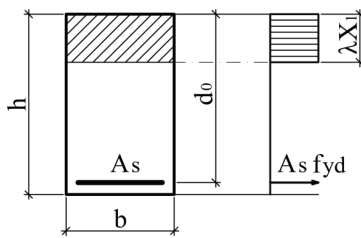


Fig. 12. The stressed-deformed state of a cross section using a rectangular diagram of the compressed zone

The resulting initial data for the calculation of an I-section are given in Table 1.

Based on these source data and by using the estimation dependences given by DSTU B V.2.6156:2010, we computed the values of stresses in concrete in the X direction and in the Y direction.

Source data for calculating an I-section	
<p>X direction</p>	<p>Y direction</p>
<p>Estimated section in the X direction</p>	<p>Estimated section in the Y direction</p>
<p>$b_w^x = 100 \text{ mm}$ $b_{eff,1}^x = 250 \text{ mm}$ $b_{eff}^x = 1100 \text{ mm}$ $h^x = 200 \text{ mm}$ $h_{eff}^x = 50 \text{ mm}$ $z_s^x = 155 \text{ mm}$ $A_s^x = 7.45 \text{ cm}^2$ Momentum $M^x = 38.9 \text{ kN}\cdot\text{m}$ Concrete, class C 20/25 Reinforcement fittings, class A400C</p>	<p>$b_w^y = 100 \text{ mm}$ $b_{eff,1}^y = 500 \text{ mm}$ $b_{eff}^y = 600 \text{ mm}$ $h^y = 200 \text{ mm}$ $h_{eff}^y = 50 \text{ mm}$ $z_s^y = 170 \text{ mm}$ $A_s^y = 3.4 \text{ cm}^2$ Momentum $M^y = 21 \text{ kN}\cdot\text{m}$ Concrete, class C 20/25 Reinforcement fittings, class A400C</p>

6. 5. Determining the stresses and estimation parameters of concrete in an I-section

The stresses in concrete were computed in line with a deformation methodology, the analytical apparatus of which was developed by the DP State Scientific and Research Institute of Building Structures (Kyiv, Ukraine) and is given in DSTU B. V.2.6-156:2010.

The concrete deformation diagram was adopted in line with expression (3.5) from DBN V.2.6-98:2009. In this expression, we substituted the characteristic value of the strength of concrete, class C20/25. The deformations ϵ_{c1} that correspond to a peak point in the diagram are taken to be equal to 0.00171, and the boundary deformations $\epsilon_{cu1} = 0.00385$. The diagram plotted in this manner (Fig. 13) was described, to simplify the integration for determining the efforts in the concrete of the compressed zone, by a fifth-degree polynomial.

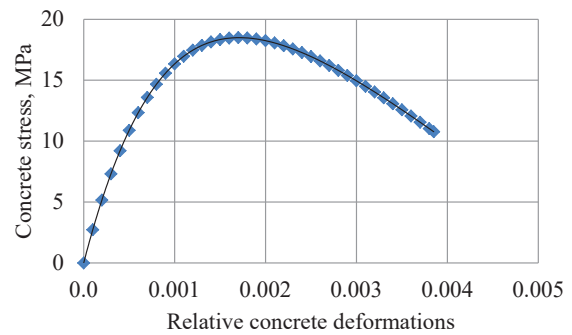


Fig. 13. Deformation diagram of concrete, class C20/25

In the slab, along the X and Y axes, the neutral axis was within the upper shelf, which is why the fourth form of equilibrium is implemented, in accordance with DSTU B V.2.6-156:2010 (Fig. 14).

Table 1

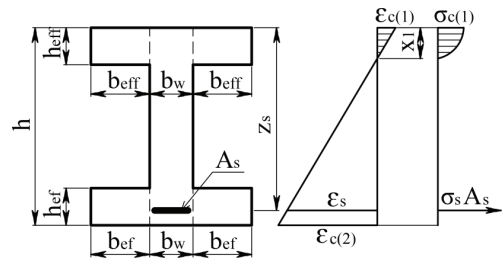


Fig. 14. Estimation diagram of an I-section

For this form of equilibrium, valid are the estimation dependences given by DSTU B V.2.6-156:2010:

$$\frac{f_{cd}}{\alpha} \left[(b_w + 2b_{eff,1}) \sum_{k=1}^5 \frac{a_k}{k+1} \left(\frac{\epsilon_{c(1)}}{\epsilon_{c1}} \right)^{k+1} \right] + \sum_{i=1}^n A_{si} \sigma_{si} - N = 0; \tag{12}$$

$$\frac{f_{cd}}{\alpha^2} \left[(b_w + 2b_{eff,1}) \sum_{k=1}^5 \frac{a_k}{k+2} \left(\frac{\epsilon_{c(1)}}{\epsilon_{c1}} \right)^{k+2} \right] + \sum_{i=1}^n A_{si} \sigma_{si} \frac{\epsilon_{c(1)} - \alpha z_{si}}{\alpha} - M = 0. \tag{13}$$

We calculated the bearing capacity of normal cross-sections using the tabular processor Excel from equations (12) and (13). Calculation results are given in Table 2.

Under the action of a bending momentum of 38.90 kN·m in the direction of the X axis, according to a deformation procedure, the height of the compressed zone $x_1=3.14$ cm, the relative deformations of reinforcement fittings are 0.0141, the extreme compressed concrete fibers – 0.0004659. These deformations correspond to the concrete stress of 10.34 MPa (Fig. 15, a).

Under the action of a bending momentum of 21 kN·m in the direction of the Y axis, according to a deformation procedure, the height of the compressed zone $x_1=3.13$ cm, the relative deformations of reinforcement fittings are 0.01694, the extreme compressed concrete fibers – 0.00038295. These deformations correspond to the concrete stress of 8.91 MPa (Fig. 15, b).

The derived values of concrete strength are used for further calculations, accepting:

$$\sigma_1 = \sigma_x = 10.34 \text{ MPa,}$$

$$\sigma_2 = \sigma_y = 8.91 \text{ MPa.}$$

To be able to apply dependences (3), (8), given by DBN V.2.6-98:2009, we shall check condition (3):

$$0 < \frac{\sigma_2}{f_{ck}} = \frac{8.91}{18.5} = 0.48 < 1.0.$$

The condition is met, so we determine the increased estimated strength of concrete from dependence (3):

$$f_{ck,c} = f_{ck} \left[1.0 + 1.38 \frac{\sigma_2}{f_{ck}} - 1.15 \left(\frac{\sigma_2}{f_{ck}} \right)^2 \right] = 18.5 \left[1.0 + 1.38 \frac{8.91}{18.5} - 1.15 \left(\frac{8.91}{18.5} \right)^2 \right] = 28.5 \text{ MPa.}$$

Relative deformations:

$$\epsilon_{c3,c} = f_{ck,c} / E_{ck,c},$$

where $\epsilon_{c3,c} = 0.71 \times 10^{-3}$ according to Table from DBN V.2.6-98:2009.

Hence,

$$E_{ck,c} = \frac{f_{ck,c}}{\epsilon_{c3,c}} = \frac{25.8}{0.71 \times 10^{-3}} = 36.3 \text{ GPa.}$$

Table 2

Results from calculating a slab in the direction of the X and Y axes in line with a deformation procedure

Calculation results in the direction of axes	$\epsilon_{c(t)}$	M , kH·m	$N = \frac{1}{p}$, 1/cm	σ_c , MPa	σ_s , kH/cm ²	M , kH·cm
X	0.0003	-0.0017	9.75E-05	7.314	-24.236	2589.925
	0.0004	-0.0022	0.00013	9.215	-31.801	3384.164
	0.0004	-0.0023	0.00014	9.739	-34.025	3616.185
	0.0005	-0.0025	0.00015	10.242	-36.228	3845.401
	0.0047	-0.0025	0.00015	10.339	-36.659	3890.155
Y	0.0003	-0.0016	9.67E-05	7.314	-26.891	1672.147
	0.0004	-0.0019	0.00011	8.295	-31.125	1931.732
	0.0004	-0.0019	0.00012	8.483	-31.964	1983.033
	0.0004	-0.002	0.00012	8.521	-32.131	1993.269
	0.0004	-0.0021	0.00012	8.908	-33.879	2100.002

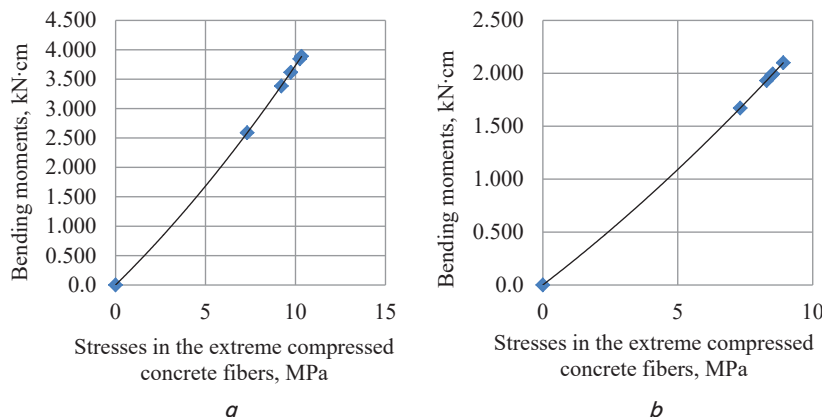


Fig. 15. Diagrams «momentum – concrete stresses» for the estimated cross-sections of a slab: a – in the direction of the X axis; b – in the direction of the Y axis

The increased values of the concrete elasticity module are used in a repeated static calculation of the flooring slab.

Our comparison of the deflections contour plots shows that due to strengthening and, accordingly, an increase in the concrete elasticity module the deflection decreased from 11.2 mm to 9.04 mm, that is by 19.3 %.

Based on the increased indicators of concrete strength, we perform checking calculations of the characteristic cross-sections of a slab for strength and crack resistance.

7. Discussion of results obtained in the calculation of slab structures

We have devised and substantiated the estimation schemes of I-sections, which are the cross-sections of slab reinforced concrete structures with the bidirectional arrangement of inserts. Compared to the generally accepted schemes reflecting the stressed state of each direction (X and Y), the devised schemes take into consideration the work of the slab reinforced concrete structures in two directions.

Based on the analysis of the stressed state, it has been shown that due to the local action of momenta in the shelves of an I-section the compressive and stretching efforts in the shelf are balan-

ced and there remain the stresses σ_x and σ_y due to the action of general momenta M_x and M_y (Fig. 3).

To determine the compressive stresses in the shelves of an I-section, we use dependences (1) and (2), which are based on the experimental-theoretical studies to which we also contributed. They reflect the fact that under the simultaneous influence of stresses in both directions (that is, at biaxial compression) the strength and rigidity of concrete significantly increase (Fig. 5, 6) – by 16...30 % and 23...56 % depending on the level of the second component of stresses in concrete. Accordingly, this positively affects the operation of slab structures that are bent in both directions.

Based on the research results, we have proposed a calculation procedure, whose special feature is the consideration of biaxial work of concrete, which is a difference in comparison with existing procedures for calculating slab structures.

The procedure is illustrated by the example of calculating an actual rectangular flooring slab in axes 3–5 between the E-G axes of the total size in plan of 6.06-6.86 m (Fig. 8). To determine the working width of the slab shelves in the X and Y directions, we applied the estimation diagrams shown in Fig. 9, 10. The bending momenta in the X and Y directions were determined by employing the software package LIRA Sapr 13 (Fig. 10, 11).

To determine the compressive stresses in the concrete of an I-section, one needs to know the amount (a cross-sectional area) of the longitudinal working reinforcement fittings, which is calculated using dependences (8) to (11).

With these initial data and the class of concrete are known (Table 1), we compute the stresses and deformability of concrete in the I-section (chapter 6.5) in line with the procedure given by DSTU B V.2.6-156:2010. According to the values derived, the concrete strength and its module of elasticity in a given example increased, respectively, by 39.4 % and 40.1 %.

The repeated general static calculation of the flooring slab, used as an example, employing the SP LIRA has shown that its deflections at the increased concrete elasticity module had decreased from 11.2 mm to 9.04 mm, that is, by 19.3 %.

The quantitative indicators of the increase in rigidity, derived from the example, should be checked by experimental studies of actual slab structures (for example, a flooring slab or its fragments).

In this case, the variables could include the general size of a flooring slab in plan and the geometric dimensions of inserts, concrete strength in the range from class 16/20 to class C25/30. It is advisable, in addition to a short-term loading, to study a long-term loading, characteristic of the actual conditions of operation for floors and other slab structures.

8. Conclusions

1. We have devised and substantiated the estimation schemes of I-sections, which are the sections of slab reinforced concrete structures with the bidirectional arrangement of inserts. Compared to the generally accepted schemes that reflect the stressed state of each direction separately, the devised schemes take into consideration the joint work of the hollow concrete slab structures in two directions, which leads to an increase in the strength and deformation characteristics of compressed concrete.

2. To determine the compressive stresses of concrete in an I-section, it has been proposed to use the dependences that are based on the experimental studies into biaxially compressed concrete to which we also contributed. According to these studies, concrete strength increases by 16...30 %, concrete deformations – by 23...56 %.

3. A procedure for calculating the hollow slab structures has been devised, taking into consideration the biaxially compressed concrete. We have given an example of calculating, in line with the proposed procedure, an actual flooring slab with inserts, which demonstrated that accounting for the biaxial strained-deformed state of concrete significantly increases the strength and rigidity of concrete in a flooring slab, by 39.4 % and 40.1 %, respectively. As a result, the deflections in an actual flooring slab, rectangular in plan, the size of 5.76-6.21 m, decreased by 19.3 %.

References

1. Melnyk, I. V., Sorokhitei, V. M., Prystavskiy, T. V. (2018). *Ploski zalizobetonni plytni konstruktsii z efektyvnymy vstavkamy*. Lviv, 272.
2. Tsvetkov, K. A., Mitrokhina, A. O. (2013). Features of the effect of dynamic loading produced on the concrete behavior at different stages of deformation caused by uniaxial and biaxial compression. *Vestnik MGSU*, 7, 77–85. doi: <https://doi.org/10.22227/1997-0935.2013.7.77-85>
3. Gang, H., Kwak, H.-G. (2017). A strain rate dependent orthotropic concrete material model. *International Journal of Impact Engineering*, 103, 211–224. doi: <https://doi.org/10.1016/j.ijimpeng.2017.01.027>
4. Quast, M., Curbach, M. (2017). Concrete under biaxial dynamic compressive loading. *Procedia Engineering*, 210, 24–31. doi: <https://doi.org/10.1016/j.proeng.2017.11.044>
5. Quast, M., Curbach, M. (2015). Behaviour of concrete under biaxial dynamic loading. *Proceeding of Fifth International Workshop on Performance, Protection and Strengthening of Structures under Extreme Loading – PROTECT*, 3–10. Available at: [https://books.google.com.ua/books?id=9c4OCgAAQBAJ&pg=PA10&lpg=PA10&dq=M.+Curbach,+M.+Quast,+Concrete+under+biaxial+impact+loading,+in:+S.+Hiermaier+\(ed.\)&source=bl&ots=e-R5fj6aOH&sig=ACfU3U170x4D0YgUj13CF-3tRP3yadvuI4A&hl=ru&sa=X&ved=2ahUKewi8itTu8NLIhVrWosKHZ__B7cQ6AEwAnoECAkQAQ#v=onepage&q=M.%20Curbach%20M.%20Quast%20Concrete%20under%20biaxial%20impact%20loading%20in%3A%20S.%20Hiermaier%20\(ed.\)&f=true](https://books.google.com.ua/books?id=9c4OCgAAQBAJ&pg=PA10&lpg=PA10&dq=M.+Curbach,+M.+Quast,+Concrete+under+biaxial+impact+loading,+in:+S.+Hiermaier+(ed.)&source=bl&ots=e-R5fj6aOH&sig=ACfU3U170x4D0YgUj13CF-3tRP3yadvuI4A&hl=ru&sa=X&ved=2ahUKewi8itTu8NLIhVrWosKHZ__B7cQ6AEwAnoECAkQAQ#v=onepage&q=M.%20Curbach%20M.%20Quast%20Concrete%20under%20biaxial%20impact%20loading%20in%3A%20S.%20Hiermaier%20(ed.)&f=true)
6. Deng, Z., Sheng, J., Wang, Y. (2018). Strength and Constitutive Model of Recycled Concrete under Biaxial Compression. *KSCE Journal of Civil Engineering*, 23 (2), 699–710. doi: <https://doi.org/10.1007/s12205-018-0575-8>

7. Ivashenko, Y., Ferder, A. (2019). Experimental studies on the impacts of strain and loading modes on the formation of concrete «stress-strain» relations. *Construction and Building Materials*, 209, 234–239. doi: <https://doi.org/10.1016/j.conbuildmat.2019.03.008>
8. Charpin, L., Le Pape, Y., Coustabeau, É., Toppani, É., Heinfling, G., Le Bellego, C. et. al. (2018). A 12 year EDF study of concrete creep under uniaxial and biaxial loading. *Cement and Concrete Research*, 103, 140–159. doi: <https://doi.org/10.1016/j.cemconres.2017.10.009>
9. Hampel, T., Speck, K., Scheerer, S., Ritter, R., Curbach, M. (2009). High-Performance Concrete under Biaxial and Triaxial Loads. *Journal of Engineering Mechanics*, 135 (11), 1274–1280. doi: [https://doi.org/10.1061/\(asce\)0733-9399\(2009\)135:11\(1274\)](https://doi.org/10.1061/(asce)0733-9399(2009)135:11(1274))
10. Rong, C., Shi, Q., Zhang, T., Zhao, H. (2018). New failure criterion models for concrete under multiaxial stress in compression. *Construction and Building Materials*, 161, 432–441. doi: <https://doi.org/10.1016/j.conbuildmat.2017.11.106>
11. Bambura, A. N., Davidenko, A. I. (1989). Eksperimental'nye issledovaniya zakonmernosti deformirovaniya betona pri dvuhosnom szhatii. *Stroitel'nye konstruksii*, 42, 95–100.
12. Mel'nyk, I. V. (2015). Analysis of the Stiffnesses of Reinforced-Concrete Plane Monolithic Floors with Tubular Inserts. *Materials Science*, 50 (4), 564–570. doi: <https://doi.org/10.1007/s11003-015-9754-7>
13. Kupfer, H., Gerstle, K. (1973). Behavior of concrete under biaxial stresses. *Journal of the Engineering Mechanics Division*, 99 (4), 853–866.
14. Gvozdev, A. A., Yashin, A. V., Petrova, K. V. et. al. (1978). Neodnoosnye napryazhenno-deformirovannyye sostoyaniya betona. Prochnost', strukturnye izmeneniya i deformatsii betona. Moscow: Stroyizdat, 196–222.
15. Bambura, A. M., Dorogova, O. V., Sazonova, I. R. (2017). Preliminary determination of the tensile reinforcement area for structures with rectangular section if bending. *Nauka ta budivnytstvo*, 3, 32–39.
16. Babaiev, V. M., Bambura, A. M., Pustovoitova, O. M. et. al. (2015). Praktychnyi rozrakhunok elementiv zalizobetonnykh konstruksiy za DBN V.2.6-98:2009 v porivnianni z rozrakhunkamy za SNyP 2.03.01-84* i EN 1992-1-1 (Eurocode 2). Kharkiv: Zoloti storinky, 240.